Enumeration of Symmetry Classes of Convex Polyominoes on the Honeycomb Lattice *

Dominique Gouyou-Beauchamps, LRI, CNRS, France
and Pierre Leroux, LaCIM, UQAM, Canada

March 9, 2004

Abstract

Hexagonal polyominoes are polyominoes on the honeycomb lattice. We enumerate the symmetry classes of *convex* hexagonal polyominoes. Here *convexity* is to be understood as convexity along the three main column directions. We deduce the generating series of *free* (i.e. up to reflection and rotation) and of *asymmetric* convex hexagonal polyominoes, according to area and half-perimeter. We give explicit formulas or implicit functional equations for the generating series, which are convenient for computer algebra.

1 Introduction

An *hexagonal polyomino* is a finite connected set of basic cells of the honeycomb lattice in the plane. Note that the hexagons of our lattice have two sides parallel to the horizontal axis. See Figure 1. Unless otherwise stated, all the polyominoes considered here are hexagonal. The *area* of a polyomino is the number of the cells composing it. Its *perimeter* is the number of line segments on its boundary. We say that a polyomino is *convex along a direction* if the intersection with any line parallel to this direction and passing through the center of a cell is connected. The convexity directions are characterized by the angle α ($0 \leq \alpha \leq \pi$) which they form with the positive horizontal axis.

Various convexity concepts have been introduced in the literature for hexagonal polyominoes, depending on the required convexity directions. Following the nomenclature of Denise, Dür, and Hassani [2], we mention the *EG-convex* polyominoes, where $\alpha = 0$ and $\pi/2$, studied by Guttmann and Enting [5] and by Lin and Chang [9], the C^1-*convex* polyominoes, where $\alpha = \pi/2$, enumerated according to many parameters by Lin and Wu [10] and by Feretić and Svrtan [4], the *strongly convex* polyominoes, where $\alpha = 0$, $\pi/3$ and $2\pi/3$, introduced by Hassani [6] and studied in [6] and [2], and finally the C- or C^3-*convex* polyominoes, where $\alpha = \pi/6$, $\pi/2$ and $5\pi/6$, introduced and enumerated according to perimeter in [6] and [2]. In particular, Hassani gives explicitly the algebraic generating function for C-convex polyominoes according to half perimeter.

It is this last class that interest us here, and that we call simply *convex polyminoes*. See Figure 1 for an example. This concept is a natural extension of (row and column) convexity on the square lattice.

*With the partial support of CNRS (France), NSERC (Canada) and FCAR (Québec). This is the full version of a paper presented at the FPSAC Conference in Vancouver, Canada, June 28 – July 2, 2004 (see [3]).

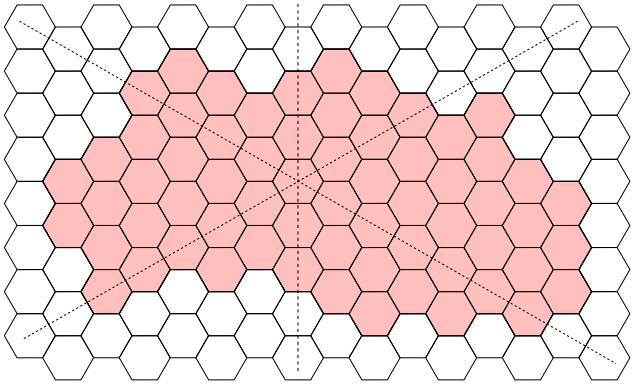

Figure 1: A convex polyomino and its convexity directions

These polyominoes are traditionally taken up to translation. However it is natural to consider them also up to rotation and reflection, as objects living freely in space. Following Vöge, Guttmann and Jensen [11], we call these equivalence classes *free polyominoes*. In organic chemistry, free polyminoes represent benzenoid hydrocarbons. See [11] where these molecules (without the convexity property) are enumerated by an exhaustive generation approach.

Our objective is to enumerate free convex polyominoes, according to area and half perimeter. Following the approach of Leroux, Rassart and Robitaille [8] for the square lattice, we consider them as orbits of the dihedral group $\mathcal{D}_6$ (the group of isometries of the regular hexagon), acting on convex polyominoes. The Cauchy-Frobenius Formula (alias Burnside's Lemma) can be used to count the orbits and we are thus lead to enumerate the symmetry classes $\mathrm{Fix}(h)$ of convex polyominoes, for each element h of the group $\mathcal{D}_6$,

It is also possible to enumerate convex polyominoes which are asymmetric or which have exactly the symmetries of a given subgroup H of $\mathcal{D}_6$, using Möbius inversion in the lattice of subgroups of $\mathcal{D}_6$. For this purpose, we also enumerate the symmetry classes $F_{\geq H}$ for each subgroup H of $\mathcal{D}_6$.

For any class $\mathcal{F}$ of convex polyominoes, we denote its generating series by $\mathcal{F}(x, q, u, v, t)$, where the variable x marks the number of columns, q marks the area, u marks the size of the first column (on the left), v, the size of the last column, and t the half perimeter; for example, the polyomino of Figure 1 has weight $x^{14}q^{64}u^2v^3t^{35}$. It is possible that some variables do not appear in some generating series. The generating series will be given by explicit formulas or implicit functional equations, which are convenient for computer algebra.

2 Preliminaries

2.1 Particular classes of convex polyominoes

Some familiar classes of convex polyominoes of the square lattice are naturally found on the honeycomb lattice and are useful. It is the case notably of *partition* and *staircase* (or *parallelogram*) polyominoes and of a variant of *stack* polyominoes.

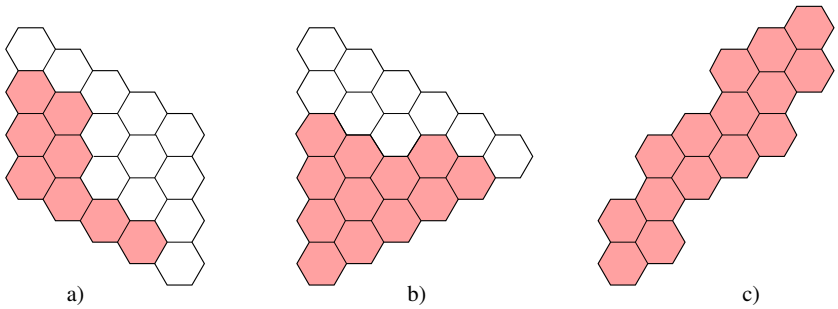

Figure 2: Partition and staircase polyominoes

2.1.1 Partition polyominoes

Figure 2a represents the partition $(4,2,2)$ contained in a *rectangle* of size 5×4 in the honeycomb lattice. Figure 2b represents the distinct part partition $(5,4,2,1)$, with parts bounded by 6. We denote by $D_m(u,q)$ the generating polynomial of distinct part partitions with parts bounded by m. Here the variable u marks the number of parts. We have

$$D_m(u,q) = (1+uq)(1+uq^2)\cdots(1+uq^m) \quad \text{and} \quad D_0(u,q) = 1. \tag{1}$$

2.1.2 Staircase polyominoes

Figure 2c represents a staircase polyomino from the square lattice (see for example [1] or [7]) redrawn on the honeycomb lattice. Observe that the half perimeter is equal to $2p-1$ where p is the half perimeter on the square lattice. We know that these polyominoes are enumerated according to half perimeter by the Catalan numbers and according to area by the sequence M1175 of [14] (A006958 of [13]) whose generating series is a quotient of two q-Bessel functions.

We denote by Pa, the set of staircase polyominoes (Pa for *Parallelogram*) on the honeycomb lattice and by $\mathrm{Pa}(x,q,u,v,t)$, their generating series. An analysis of the situation where a column is added on the right, following the method of M. Bousquet-Melou (compare with [1], Lemma 3.1), gives, for $\mathrm{Pa}(v) = \mathrm{Pa}(x,q,u,v,t)$,

$$\mathrm{Pa}(v) = \frac{xquvt^3}{1-quvt^2} + \frac{xqvt^2}{(1-qvt^2)(1-qv)}\left(\mathrm{Pa}(1) - \mathrm{Pa}(vq)\right) \tag{2}$$

so that

$$\mathrm{Pa}(v) = \frac{J_1(1) + J_1(v)J_0(1) - J_1(1)J_0(v)}{J_0(1)}, \tag{3}$$

where

$$J_1(v) = \sum_{n\geq 0}(-1)^n \frac{x^{n+1}v^{n+1}ut^{2n+3}q^{\binom{n+2}{2}}}{(qvt^2;q)_n(qv;q)_n(1-q^{n+1}uvt^2)}$$

and

$$J_0(v) = \sum_{n\geq 0}(-1)^n \frac{x^n v^n t^{2n} q^{\binom{n+1}{2}}}{(qvt^2;q)_n(qv;q)_n}.$$

Here we have used the familiar notation $(a;q)_n = (1-a)(1-aq)\cdots(1-aq^{n-1}$. We set

$$\mathrm{Pa}(x,q,u,v,t) = \sum_{i\geq 1\, j\geq 1} \mathrm{Pa}_{i,j}(x,q,t)u^i v^j. \tag{4}$$

2.1.3 Stack polyominoes

There exists a specific variant of stack polyominoes on the honeycomb lattice. They consist of pyramidal stackings of hexagons, viewed sideways for our purposes. A first class (see Figure 3a), denoted by T (for French *tas*), appears in the literature under the name of *pyramidal stacking of circles*; see [12]. Their generating series according to area is referenced as number M0687 in [14] and A001524 in [13].

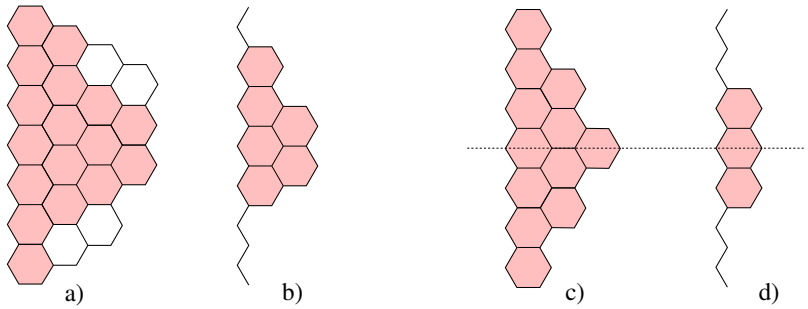

Figure 3: Stacks and symmetric stacks

Let $T(x, u, q)$ be the generating series of stack polyominoes according to the number of columns (the *width*, marked by x), the size of the first column (the *height*, marked by u) and the area, and let $T_n(x, q) = [u^n]T(x, u, q)$ be the generating series of stacks whose first column is of size n. Note that the half perimeter is equal to twice the height plus the width so that the series $T(xt, ut^2, q)$ also keeps track of this parameter.

We have

$$T(x, u, q) = \sum_{m\geq 1} \frac{x^m q^{\binom{m+1}{2}} u^m}{((uq; q)_{m-1})^2 (1 - uq^m)} \tag{5}$$

and

$$T_n(x, q) = \sum_{m=1}^{n} x^m q^{n+\binom{m}{2}} \sum_{j=0}^{n-m} \begin{bmatrix} m+j-1 \\ m-1 \end{bmatrix}_q \begin{bmatrix} n-j-2 \\ m-2 \end{bmatrix}_q . \tag{6}$$

The polynomials $T_n(x, q)$ can also be rapidly computed by recurrence using the class $\mathrm{T0}_n$ of stack polyominoes whose first column is of size n, including empty cells at the two extremities. See Figure 3b. Indeed, we have

$$T_n(x, q) = xq^n \mathrm{T0}_{n-1}(x, q). \tag{7}$$

with $\mathrm{T0}_0(x, q) = 1$, $\mathrm{T0}_1(x, q) = 1 + xq$, and, arguing on the existence of empty cells at each extremity,

$$\mathrm{T0}_n(x, q) = (2 + xq^n)\mathrm{T0}_{n-1} - \mathrm{T0}_{n-2}, \tag{8}$$

2.1.4 Symmetric stacks

Horizontally symmetric stacks (see Figures 3c and 3d), constitute the families TS and TS0. Using the same notation as for stacks, we have

$$\mathrm{TS}(x, u, q) = \sum_{m\geq 1} \frac{x^m u^m q^{m(m+1)/2}(1 + uq^m)}{(1 - u^2q^2)(1 - u^2q^4) \cdots (1 - u^2q^{2m})}. \tag{9}$$

Moreover,

$$\mathrm{TS}_n(x,q) = xq^n \mathrm{TS0}_{n-1}(x,q). \tag{10}$$

where $\mathrm{TS0}_0(x,q) = \mathrm{TS0}_{-1}(x,q) = 1$, and

$$\mathrm{TS0}_n(x,q) = xq^n \mathrm{TS0}_{n-1}(x,q) + \mathrm{TS0}_{n-2}(x,q), \tag{11}$$

2.2 The dihedral group $\mathcal{D}_6$

The dihedral group $\mathcal{D}_6$ is defined algebraically by

$$\mathcal{D}_6 = \langle \rho, \tau \mid \rho^6 = 1,\ \tau^2 = 1,\ \tau\rho\tau = \rho^{-1} \rangle.$$

Here $\mathcal{D}_6$ is realized as the group of isometries of a regular hexagon, with $\rho = \mathrm{r}$ = the (clockwise) rotation of $\pi/3$ radian and $\tau = \mathrm{ds}_3 = \mathrm{h}$, the horizontal reflection. We have

$$\mathcal{D}_6 = \{\mathrm{id}, \mathrm{r}, \mathrm{r}^2, \mathrm{r}^3, \mathrm{r}^4, \mathrm{r}^5, \mathrm{da}_1, \mathrm{da}_2, \mathrm{da}_3, \mathrm{ds}_1, \mathrm{ds}_2, \mathrm{ds}_3\},$$

where $\mathrm{ds}_2 = \tau\mathrm{r}^2$, $\mathrm{ds}_1 = \tau\mathrm{r}^4$, reflections according to vertex-vertex axes, and $\mathrm{da}_3 = \tau\mathrm{r}$, $\mathrm{da}_2 = \tau\mathrm{r}^3$, and $\mathrm{da}_1 = \tau\mathrm{r}^5$, reflections according to the edge-edge axes. See Figure 4.

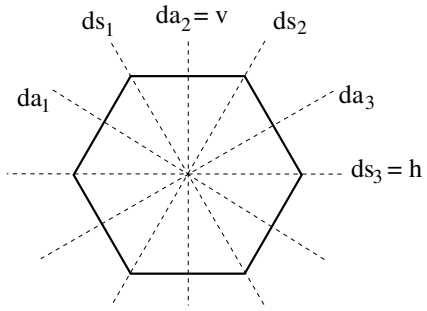

Figure 4: The reflections of $\mathcal{D}_6$

The dihedral group $\mathcal{D}_6$ acts naturaly on (hexagonal) polyominoes, by rotation or reflection. For any class $\mathcal{F}$ of polyominoes, with a monomial weigh w corresponding to certain parameters, we denote by $|\mathcal{F}|_w$ the total weight (i.e. the generating series) of this class. If $\mathcal{F}$ is invariant under the action of $\mathcal{D}_6$, then the set of orbits of this action is denoted by $\mathcal{F}/\mathcal{D}_6$. Burnside's Lemma enumerates these orbits in terms of the sets $\mathrm{Fix}(g)$ of fixed points of each of the elements g of $\mathcal{D}_6$, the *symmetry classes* of $\mathcal{F}$. We write $\mathrm{fix}(g) = |\mathrm{Fix}(g)|_w$. Clearly we have $\mathrm{fix}(\mathrm{r}) = \mathrm{fix}(\mathrm{r}^5)$, $\mathrm{fix}(\mathrm{r}^2) = \mathrm{fix}(\mathrm{r}^4)$ and, for symmetry reasons, $\mathrm{fix}(\mathrm{da}_1) = \mathrm{fix}(\mathrm{da}_2) = \mathrm{fix}(\mathrm{da}_3)$ and $\mathrm{fix}(\mathrm{ds}_1) = \mathrm{fix}(\mathrm{ds}_2) = \mathrm{fix}(\mathrm{ds}_3)$. In the following, we will choose $\mathrm{v} = \mathrm{da}_2$, the vertical axis, and $\mathrm{h} = \mathrm{ds}_3$, the horizontal axis. We then have

$$\begin{aligned} |\mathcal{F}/\mathcal{D}_6|_w &= \frac{1}{12} \sum_{g \in \mathcal{D}_6} \mathrm{fix}(g) \\ &= \frac{1}{12} \Big(|\mathcal{F}|_w + 2\,\mathrm{fix}(\mathrm{r}) + 2\,\mathrm{fix}(\mathrm{r}^2) + \mathrm{fix}(\mathrm{r}^3) + 3\,\mathrm{fix}(\mathrm{v}) + 3\,\mathrm{fix}(\mathrm{h}) \Big). \end{aligned} \tag{12}$$

2.2.1 The lattice of subgroups of $\mathcal{D}_6$

It is also possible to enumerate the convex polyominoes which are *asymmetric* or which have exactly the symmetries of a given subgroup H of $\mathcal{D}_6$, with the help of Möbius inversion in the lattice of subgroups of $\mathcal{D}_6$. This lattice and its Möbius function are well described in Stockmeyer's Ph.D. thesis [15], for any dihedral group $\mathcal{D}_n$. We follow his nomenclature. Apart from the trivial subgroups $0 = \{\mathrm{id}\}$ and $1 = \mathcal{D}_6 =< \mathrm{r}, \mathrm{h} >$, we have the cyclic subgroups

$$C_6 =< \mathrm{r} >= \{1, \mathrm{r}, \mathrm{r}^2, \mathrm{r}^3, \mathrm{r}^4, \mathrm{r}^5\}, \quad C_3 =< \mathrm{r}^2 >= \{1, \mathrm{r}^2, \mathrm{r}^4\} \quad \text{and} \quad C_2 =< \mathrm{r}^3 >= \{1, \mathrm{r}^3\},$$

$$F_{1,1} =< \mathrm{ds}_2 >= \{1, \mathrm{ds}_2\}, \quad F_{1,2} =< \mathrm{ds}_1 >= \{1, \mathrm{ds}_1\} \quad \text{and} \quad F_{1,3} =< \mathrm{h} >= \{1, \mathrm{h}\},$$

$$H_{1,1} =< \mathrm{da}_3 >= \{1, \mathrm{da}_3\}, \quad H_{1,2} =< \mathrm{v} >= \{1, \mathrm{v}\} \quad \text{and} \quad H_{1,3} =< \mathrm{da}_1 >= \{1, \mathrm{da}_1\},$$

as well as the two generator subgroups

$$F_{3,1} =< \mathrm{r}^2, \mathrm{ds}_2 >= \{1, \mathrm{r}^2, \mathrm{r}^4, \mathrm{ds}_1, \mathrm{ds}_2, \mathrm{h}\} =< \mathrm{r}^2, \mathrm{h} >,$$

$$H_{3,1} =< \mathrm{r}^2, \mathrm{da}_3 >= \{1, \mathrm{r}^2, \mathrm{r}^4, \mathrm{da}_1, \mathrm{v}, \mathrm{da}_3\} =< \mathrm{r}^2, \mathrm{v} >,$$

and the $D_{2,j} =< \mathrm{r}^3, \tau\mathrm{r}^{2j} >$, $j = 1, 2, 3$, that is

$$D_{2,1} =< \mathrm{r}^3, \mathrm{ds}_2 >= \{1, \mathrm{r}^3, \mathrm{ds}_2, \mathrm{da}_1\}, \qquad D_{2,2} =< \mathrm{r}^3, \mathrm{ds}_1 >= \{1, \mathrm{r}^3, \mathrm{ds}_1, \mathrm{da}_3\},$$

$$\text{and} \quad D_{2,3} =< \mathrm{r}^3, \mathrm{h} >= \{1, \mathrm{r}^3, \mathrm{h}, \mathrm{v}\} =< \mathrm{r}^3, \mathrm{h} > .$$

The lattice of subgroups of $\mathcal{D}_6$ is represented in Figure 5.

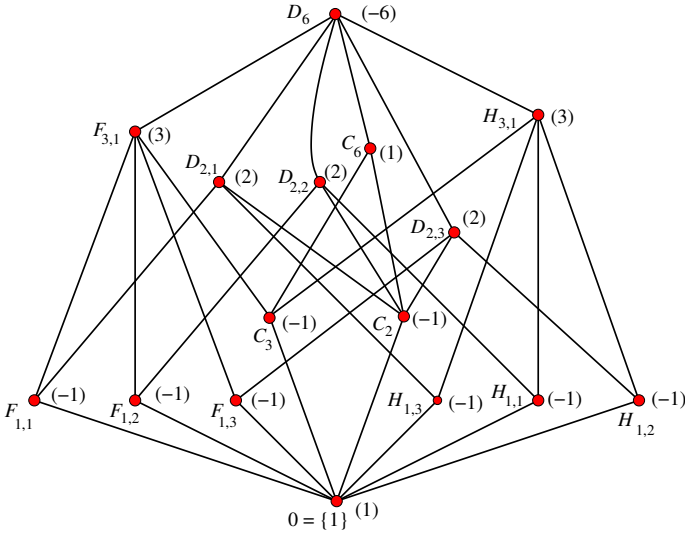

Figure 5: The lattice of subgroups of D_6 ($\mu(0, H)$ in parenthesis)

For any subgroup H of $\mathcal{D}_6$ ($H \leq \mathcal{D}_6$), we set

$$F_{\geq H} = |\{s \in \mathcal{F} \mid \mathrm{stab}(s) \geq H\}|_w = |\{s \in \mathcal{F} \mid h \in H \Rightarrow h \cdot s = s\}|_w \tag{13}$$

and

$$F_{=H} = |\{s \in \mathcal{F} \mid \mathrm{stab}(s) = H\}|_w = |\{s \in \mathcal{F} \mid h \in H \Leftrightarrow h \cdot s = s\}|_w \tag{14}$$

We have clearly, for any $H \leq \mathcal{D}_6$

$$F_{\geq H} = \sum_{H \leq K \leq \mathcal{D}_6} F_{=K}$$

and, by Möbius inversion,

$$F_{=H} = \sum_{H \leq K \leq \mathcal{D}_6} \mu(H,K) F_{\geq K}$$

In particular, the total weight of asymmetric polyominoes is given by

$$F_{=0} = \sum_{K \leq \mathcal{D}_6} \mu(0,K) F_{\geq K} \tag{15}$$

Note that $F_{\geq 0} = |\mathcal{F}|_w$ and that for any cyclic subgroup $H =< h >$, $F_{\geq H} = \mathrm{fix}(h)$. For reasons of symmetry (or by conjugation), we have $F_{\geq D_{2,1}} = F_{\geq D_{2,2}} = F_{\geq D_{2,3}}$. In the following, we will take $D_{2,3} =< \mathrm{r}^3, \mathrm{h} >$. The formula (15) then yields

$$F_{=0} = |\mathcal{F}|_w - 3\,\mathrm{fix(h)} - 3\,\mathrm{fix(v)} - \mathrm{fix}(\mathrm{r}^2) - \mathrm{fix}(\mathrm{r}^3) + \mathrm{fix(r)} + 6F_{\geq D_{2,3}} + 3F_{\geq F_{3,1}} + 3F_{\geq H_{3,1}} - 6F_{\geq \mathcal{D}_6}. \tag{16}$$

For any subgroup H of $\mathcal{D}_6$, we sometimes write $|\mathrm{Fix}(H)|_{q,t} = F_{\geq H}$ when the weight is given by the area and the half perimeter.

2.3 Growth phases of convex polyominoes

Any convex polyomino can be decomposed into blocks according to the growth phases, from left to right, of its upper and lower profiles. Figure 6 gives an example of this decomposition. The upper profile is represented by the path from A to B along the upper boundary, and the lower profile, by the path from C to D. On the upper profile, we speak of a *weak growth* if the level rises by a half hexagon only with respect to the preceding column, and of a *strong* growth if the level rises by more than a half hexagon. We define analogously a *weak* or *strong decrease*. On the lower profile, a growth corresponds to a descent and a decrease, to a rise.

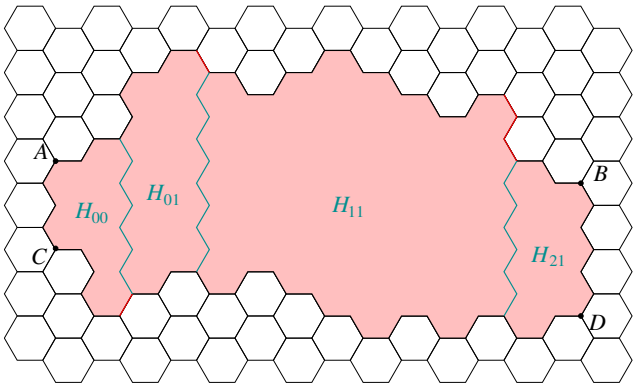

Figure 6: Growth phases of a convex polyomino

The state in which a column lies is described by an ordered pair (i,j), $i,j = 0,1,2$; the first component corresponds to the upper profile and the second, to the lower profile. The state 0

corresponds to a (weak or strong) growth, at the start of the polyomino, the state 1 to a weak growth or decrease, in an oscillation phase, and the state 2, to a strong or weak decrease, in the last part of the polyomino. To pass from the state 0 to the state 1, there must be a first weak decrease, and to pass from the state 0 or 1 to the state 2, there must be a strong decrease. Finally, the transitions from the state 1 to the state 0 and from the state 2 to the state 1 or 0 are impossible. Now, a block H_{ij} is characterized by a maximal sequence of consecutive columns which are in the state (i, j).

We can then view a convex polyomino as an assemblage of blocks and we will first enumerate these blocks H_{ij}. In what follows, we give the various generating series of the form $H_{ij}(x, q, u, v, t)$.

2.3.1 The families H_{00} and H_{22}

The polyominoes of the classes H_{00} and H_{22} are easy to enumerate for they are in fact stack polyominoes. Here, only one of the two variables u and v is used at a time. We have

$$H_{22}(x, q, u, t) = T(xt, ut^2, q) \quad \text{and} \quad H_{00}(x, q, v, t) = T(xt, vt^2, q), \tag{17}$$

where $T(x, u, q)$ is given by (5).

2.3.2 The families H_{01}, H_{10}, H_{12}, and H_{21}

The classes H_{01}, H_{10}, H_{12}, and H_{21} of polyominoes are in bijection with each other by horizontal and vertical reflections and are thus equinumerous. Figure 7 shows a polyomino in H_{10}. We easily find that

$$H_{10}(x, q, u, v, t) = \frac{xquvt^3}{1 - quvt^2} + \frac{xt^2(1 + qvt)}{1 - qvt^2} H_{10}(x, q, u, vq, t) \tag{18}$$

$$= \sum_{m \geq 1} \frac{x^m q^m uvt^{2m+1}(-qvt; q)_{m-1}}{(qvt^2; q)_{m-1}(1 - q^m uvt^2)}. \tag{19}$$

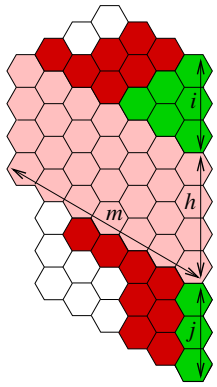

Figure 7: Polyomino of H_{10}

Formula (19) can be seen directly on Figure 7. We also see that

$$H_{10}(x,q,u,v,t) = \sum_{h\geq 1} u^h v^h \sum_{m\geq 1} x^m q^{mh} \sum_{i=0}^{m-1} v^i q^{\binom{i+1}{2}} \begin{bmatrix} m-1 \\ i \end{bmatrix}_q \sum_{j\geq 0} v^j q^j t^{2m+2h+i+2j-1} \begin{bmatrix} m-2+j \\ j \end{bmatrix}_q . \tag{20}$$

Note that $H_{01}(x,q,u,v,t) = H_{10}(x,q,u,v,t)$ and that $H_{12}(x,q,u,v,t) = H_{21}(x,q,u,v,t) = H_{10}(x,q,v,u,t)$.

2.3.3 The families H_{02} and H_{20}

These two classes are in fact equivalent to staircase polyominoes:

$$H_{02}(x,q,u,v,t) = \mathrm{Pa}(x,q,u,v,t) = H_{20}(x,q,u,v,t). \tag{21}$$

2.3.4 The family H_{11}

The class H_{11} contains the convex polyominoes whose upper and lower profiles are both oscillating. When we examine the diagonal row of hexagons in the da_3 axis (see Fig. 4) containing the first column's lower cell, two subclasses of H_{11} appear. In the first class, denoted by H_{11a}, this diagonal row and those to its right (up to the last column) form a staircase polyomino (rotated clockwise by a $\pi/3$ angle); see Figure 8a. In the second class, denoted by H_{11b}, this diagonal is the basis of a rectangle of height at least 2; see Figure 8b. In both cases, we find, above and below these objects (staircase or rectangle), distinct part partitions which are left and right justified, respectively.

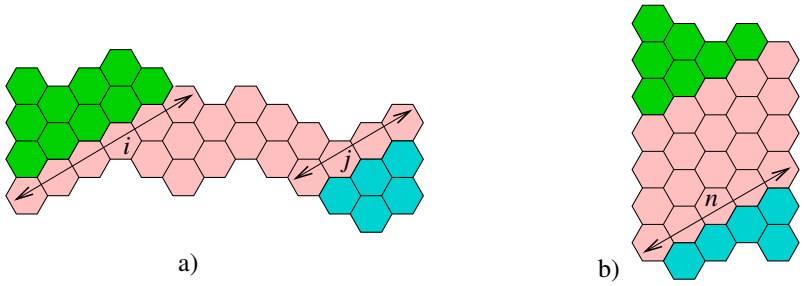

Figure 8: Polyominoes of H_{11}

Recall that in the series $\mathrm{Pa}_{i,j}(x,q,t)$, defined by (4), the variable x marks the number of columns of the (unrotated) staircase polyomino. We rather use the link between its width ℓ, when rotated, and its half-perimeter p: $p = 2\ell + 1$. Hence we have

$$H_{11}(x,q,u,v,t) = H_{11a}(x,q,u,v,t) + H_{11b}(x,q,u,v,t) \tag{22}$$

with

$$H_{11a}(x,q,u,v,t) = \sum_{i\geq 1\, j\geq 1} x^{-\frac{1}{2}} uv\, \mathrm{Pa}_{i,j}(1,q,tx^{\frac{1}{2}}) D_{i-1}(ut,q) D_{j-1}(vt,q) \tag{23}$$

and

$$H_{11b}(x,q,u,v,t) = \sum_{n\geq 1} \frac{x^n q^{2n} u^2 v^2 t^{2n+3} D_{n-1}(ut,q) D_{n-1}(vt,q)}{1-q^n uvt^2}. \tag{24}$$

3 Convex and directed convex polyominoes

3.1 Convex polyominoes

We denote by C, the class of all convex polyominoes and by C_{ij}, the subclass of polyominoes whose last column is in the state (i,j), $i,j=0,1,2$. This determines a partition of C. To enumerate C, we must enumerate each of the classes C_{ij}. We give the generating series $C_{ij}(x,q,v,t)$, using the growth phase decomposition of a convex polyomino, following essentially the method of Hassani [6].

We use the notation $C_{ij}\otimes H_{i'j'}$ for the set of convex polyominoes obtained by gluing together in all the possible ways a polyomino of C_{ij} with one of $H_{i'j'}$. We introduce the series $C_{ij,n}(x,q,t)$ and $H_{ij,n}(x,q,v,t)$ by the coefficient extractions

$$C_{ij,n}(x,q,t)=[v^n]C_{ij}(x,q,v,t) \quad \text{and} \quad H_{ij,n}(x,q,v,t)=[u^n]H_{ij}(x,q,u,v,t). \tag{25}$$

For example, we have $C_{00}=H_{00}$, $C_{10}=C_{00}\otimes H_{10}$ and

$$\begin{aligned} C_{10}(x,q,v,t) &= \sum_{n\geq 1}\left(\sum_{k=1}^{n}\frac{1}{t^{2k-1}}C_{00,k}(x,q,t)\right)H_{10,n}(x,q,v,t) \\ &= \sum_{n\geq 1}\left(\sum_{k=1}^{n}tT_k(xt,q)\right)H_{10,n}(x,q,v,t) \\ &= C_{01}(x,q,v,t). \end{aligned} \tag{26}$$

Likewise, $C_{11}=(C_{00}+C_{10}+C_{01})\otimes H_{11}=C_{00}\otimes H_{11}+C_{10}\otimes H_{11}+C_{01}\otimes H_{11}$ and

$$C_{00}\otimes H_{11}\,(x,q,v,t)=\sum_{n\geq 2}\frac{1}{t^{2n-2}}C_{00,n}(x,q,t)H_{11,n-1}(x,q,v,t), \tag{27}$$

$$C_{10}\otimes H_{11}\,(x,q,v,t)=\sum_{n\geq 1}\frac{1}{t^{2n-1}}C_{10,n}(x,q,t)H_{11,n}(x,q,v,t)+\sum_{n\geq 2}\frac{1}{t^{2n-2}}C_{10,n}(x,q,t)H_{11,n-1}(x,q,v,t). \tag{28}$$

We have also $C_{02}=(C_{00}+C_{01})\otimes H_{02}$,

$$C_{12}=(C_{00}+C_{01}+C_{10}+C_{11}+C_{02})\otimes H_{12},$$

$$C_{22}=(C_{00}+C_{01}+C_{10}+C_{11}+C_{02}+C_{02})\otimes H_{22}.$$

Finally,

$$C(x,q,v,t)=(C_{00}+2C_{10}+C_{11}+2C_{02}+2C_{12}+C_{22})(x,q,v,t). \tag{29}$$

3.2 Directed convex polyominoes

There is a special class of convex polyominoes which will be particularly useful in the following, namely those which are directed according to the North direction with a diagonal basis. See Figure 9. We call them simply *directed convex*, and denote this class by $\mathcal{D}$.

Analogously to convex polyominoes, any polyomino in $\mathcal{D}$ can be decomposed into blocks H_i according to the growth phases $i=0,1,$ ou 2, of its upper profile. Their generating series can be computed directly by observation. Since the half perimeter can be deduced from the other

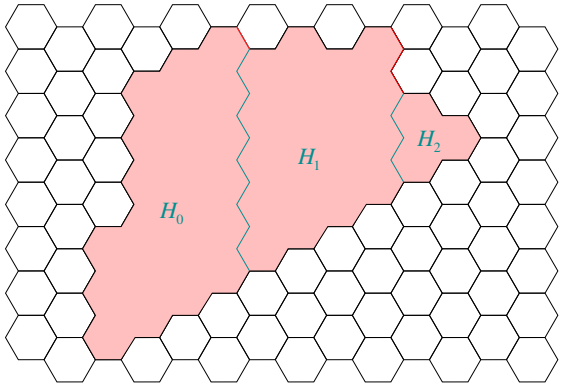

Figure 9: Directed convex polyomino

parameters, the variable t does not appear here. For example, a polyomino in H_0 is identified with a partition and we find

$$H_0(x,q,v) = \sum_{l\geq 1}\sum_{k\geq 1} v^l x^k q^{l+k} \begin{bmatrix} l+k-2 \\ l-1 \end{bmatrix}_q . \tag{30}$$

A polyomino in H_1 can be decomposed into pieces as shown in Figure 10a, yielding

$$H_1(x,q,u,v) = \sum_{l\geq 1} v^l \sum_{m\geq 0} u^{l+m} \sum_{k\geq m+1} x^k q^{kl+\frac{(m)(m+1)}{2}} \begin{bmatrix} k-1 \\ m \end{bmatrix}_q . \tag{31}$$

Likewise, for H_2, we find (see Figure 10b)

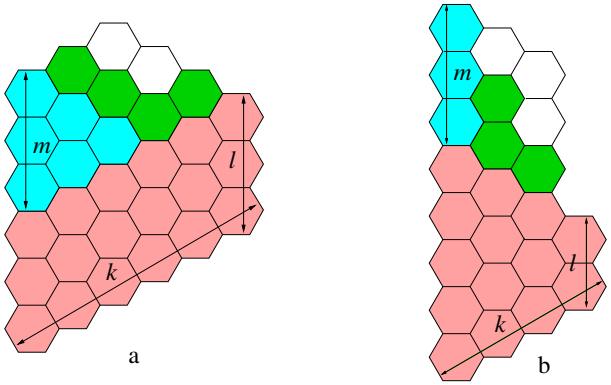

Figure 10: Directed convex polyominos in H_1 and in H_2

$$H_2(x,q,u,v) = \sum_{l\geq 1} v^l \left(xq^l u^l + \sum_{k\geq 2} x^k \sum_{m\geq 0} u^{l+k+m-1} q^{\frac{k(k+2l-1)}{2}+m} \begin{bmatrix} m+k-2 \\ k-2 \end{bmatrix}_q \right). \tag{32}$$

We denote by $\mathcal{D}_i$, the class of directed convex polyominoes whose last column is in the state $i,\ i = 0,1,2$, and we introduce the notation

$$\mathcal{D}_{i,n}(x,q,t) = [v^n]\mathcal{D}_i(x,q,v,t) \quad \text{and} \quad H_{i,n}(x,q,v) = [u^n]H_i(x,q,u,v). \tag{33}$$

We have

$$\mathcal{D}_0(x,q,v,t) = \frac{1}{t}H_0(xt^2,q,vt^2), \tag{34}$$

$\mathcal{D}_1 = \mathcal{D}_0 \otimes H_1$ and

$$\mathcal{D}_1(x,q,v,t) = \sum_{m\geq 1}\frac{1}{t^m}\mathcal{D}_{0,m+1}(x,q,t)H_{1,m}(xt^2,q,vt), \tag{35}$$

and finally, $\mathcal{D}_2 = (\mathcal{D}_0 + \mathcal{D}_1) \otimes H_2$ and

$$\mathcal{D}_2(x,q,v,t) = \sum_{m\geq 1}\sum_{h\geq 2}\frac{1}{t^m}(\mathcal{D}_{0,m+h}(x,q,t) + \mathcal{D}_{1,m+h}(x,q,t))H_{2,m}(xt^2,q,vt). \tag{36}$$

4 Reflexive symmetry classes

4.1 Vertical symmetry

Consider a vertically symmetric (v-symmetric) convex polyomino P. We see that the symmetry axis goes through a central column. Denote by K the left fundamental region of P, including the central column. See Figure 11. We have

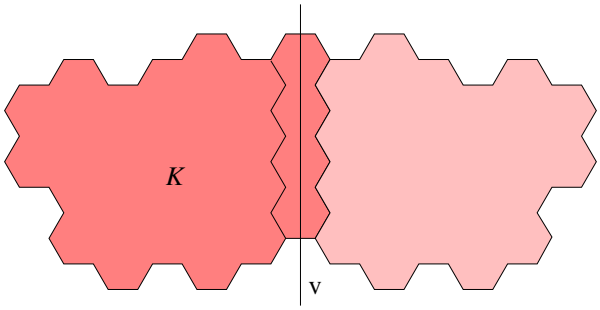

Figure 11: Polyomino convex v-symmetric

$$\begin{aligned} K(x,q,v,t) &= C_{00}(x,q,v,t) + 2C_{10}(x,q,v,t) + C_{11}(x,q,v,t) \\ &= \sum_{m\geq 1} K_m(x,q,t)v^m \end{aligned} \tag{37}$$

and

$$|\mathrm{Fix(v)}|_{q,t} = \sum_{m\geq 1}\frac{1}{q^m t^{2m+1}}K_m(1,q^2,t^2). \tag{38}$$

4.2 Horizontal symmetry

The class S of h-symmetric convex polyominoes is partitioned into three classes: S_a and S_b, wether or not we can find an *arrowhead* polyomino in the oscillating part (see Figures 12a and 12b) and the class S_c, if there does not exist an oscillating part.

In order to construct a polyomino of the class *arrrowhead*, denoted by A, we start with a triangle of side n, to which a symmetric stack is possibly attached to form the H_{22} phase; denote

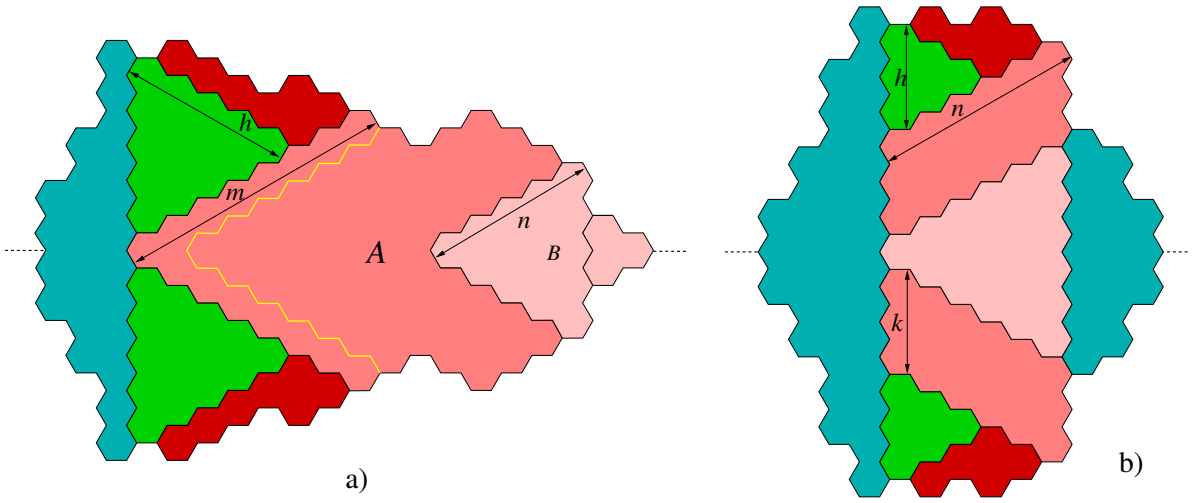

Figure 12: h-symmetric convex polyominoes

by B, this starting class of polyominoes. From B, we construct A by successively attaching V-shaped bands on the left, as illustrated in Figure 12a. Let the variable s mark the size of the last attached V's upper left part. We have

$$B(s,x,q,t) = sxqt^3 + \sum_{n\geq 2} s^n x^n q^{n(n+1)/2} t^{3n} \mathrm{TS0}_{n-3}(xt,q) \tag{39}$$

and the generating series $A(s) = A(s,x,q,t)$ is characterized by the following functional equation, which can be solved by the usual method:

$$A(s) = B(s) + \frac{s^2x^2q^3t^4}{1-sq^2}A(1) - A(sq^2). \tag{40}$$

We set $A(s,x,q,t) = \sum_{m\geq 1} A_m(x,t,q)s^m$. To complete the polyomino, we must take into account the parity of the first oscillating column. The first case, illustrated in Figure 12a, is when this column is of odd size. In the second case, this even column is placed in front of the arrrowhead. In conclusion, we obtain

$$\begin{aligned} S_a(x,t,q) &= \sum_{h\geq 0} q^{h(h+1)} t^{2h+2} \mathrm{TS}_{2h+2}(xt,q) \sum_{m\geq h+1} \begin{bmatrix} m-1 \\ h \end{bmatrix}_{q^2} A_m(x,t,q) \\ &\quad + \sum_{h\geq 1} q^{h(h+1)} t^{2h+3} \mathrm{TS}_{2h+1}(xt,q) \sum_{m\geq h} \begin{bmatrix} m \\ h \end{bmatrix}_{q^2} A_m(x,t,q). \end{aligned} \tag{41}$$

The computations for $S_b(x,t,q)$ and $S_c(x,t,q)$ are simpler. For S_b, there are also two parity cases and we find directly

$$\begin{aligned} S_b(x,t,q) &= \sum_{n\geq 1} x^n q^{\binom{n+1}{2}} t^{3n} \sum_{k\geq 1} q^{2kn} t^{4k} \mathrm{TS0}_{n+2k-3}(xt,q) \sum_{h=0}^{n-1} t^{2h+2} q^{h(h+1)} \begin{bmatrix} n-1 \\ h \end{bmatrix}_{q^2} \mathrm{TS}_{2k+2h+2}(x,t,q) \\ &\quad + \sum_{n\geq 0} x^n q^{\binom{n+1}{2}} t^{3n} \sum_{k\geq 1} q^{2k(n+1)} t^{4k+1} \mathrm{TS0}_{n+2k-3}(xt,q) \sum_{h=0}^{n} t^{2h+2} q^{h(h+1)} \begin{bmatrix} n \\ h \end{bmatrix}_{q^2} \mathrm{TS}_{2k+2h+1}(x,t,q) \end{aligned} \tag{42}$$

and

$$S_c(x,t,q) = \sum_{h\geq 1} t^{2h}\mathrm{TS}_h(xt,q)\mathrm{TS0}_{h-3}(xt,q). \tag{43}$$

Finally,

$$|\mathrm{Fix(h)}|_{q,t} = S_a(1,t,q) + S_b(1,t,q) + S_c(1,t,q). \tag{44}$$

5 Rotational symmetry classes

5.1 Symmetry with respect to the $\pi/3$ radian rotation r

The polyominoes which are symmetric with respect to the $\pi/3$ rotation (r-symmetric) are essentially formed of large hexagons decorated by stack polyominoes of the class T0. We find

$$|\mathrm{Fix(r)}|_{q,t} = \sum_{h\geq 1} t^{3(2h-1)}q^{3h(h-1)+1}\mathrm{T0}_{h-1}(t^6,q^6), \tag{45}$$

the series $\mathrm{T0}_n(x,q)$ being defined by (8).

5.2 Symmetry with respect to the $2\pi/3$ radian rotation r^2

The situation is more complex here. First we must distinguish the case where the rotation center is in the middle of an hexagon from the one where it is on a vertex. This determines two subclasses, denoted by $\mathcal{P}$ and $\mathcal{Q}$.

5.2.1 The rotation center is in the middle of an hexagon

When the rotation center is in the middle of an hexagon, we consider the fundamental region formed by the upper third of the r^2-symmetric polyomino. The parameters h_1 and h_2 are defined as the extent of the fundamental region in the directions $\mathrm{da}_2 = \mathrm{v}$ and da_1 (or da_3), respectively. There are three subcases according to wether $h_1 > h_2$, $h_2 > h_1$ or $h_1 = h_2$, giving three subclasses denoted by $\mathcal{P}_1$, $\mathcal{P}_2$ and $\mathcal{P}_3$. Figure 13 illustrates the first subcase $\mathcal{P}_1$.

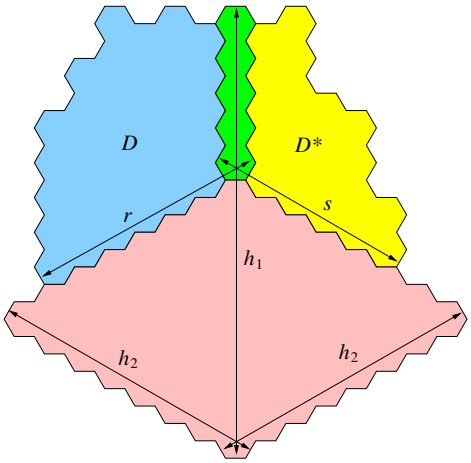

Figure 13: Fundamental region of an r^2-symmetric convex polyomino in $\mathcal{P}_1$

In this figure, there is a basis formed of (one third of) a super-hexagon of *radius* $h = h_2$, on top of which are placed a directed convex polyomino D (see the subsection 3.2) and the image D^* under v of another directed convex polyomino, these two polyominoes sharing a common column. Let ℓ be the size of this common column, so that $h_1 = h + \ell$. We must consider all such legal combinations $\mathcal{D} \otimes \mathcal{D}^*$ and take into account the added area and half perimeter over that of the super-hexagon. For $i = 0, 1, 2$, we set

$$\mathcal{D}_{i,r,n}(q,t) = \frac{1}{t^{2r+n-1}}[x^r]\mathcal{D}_{i,n}(x,q,t) = \frac{1}{t^{2r+n-1}}[x^r][v^n]\mathcal{D}_i(x,q,v,t)$$

and $\mathcal{D}_{r,n}(q,t) = (\mathcal{D}_{0,r,n} + \mathcal{D}_{1,r,n} + \mathcal{D}_{2,r,n})(q,t)$. We then have

$$\begin{aligned}\mathcal{P}_1(q,t) \;=\; & \sum_{h\geq 1} t^{3(2h-1)} q^{3h(h-1)+1} \\ & \sum_{l\geq 1}\sum_{r=1}^{h}\sum_{s=1}^{h} \frac{1}{q^{3l}} \Big(\mathcal{D}_{0,r,l}(q^3,t^3)\mathcal{D}_{0,s,l}(q^3,t^3) + 2\mathcal{D}_{0,r,l}(q^3,t^3)\mathcal{D}_{1,s,l}(q^3,t^3) + \\ & 2\mathcal{D}_{0,r,l}(q^3,t^3)\mathcal{D}_{2,s,l}(q^3,t^3) + \mathcal{D}_{1,r,l}(q^3,t^3)\mathcal{D}_{1,s,l}(q^3,t^3)\Big). \quad (46)\end{aligned}$$

For reasons of symmetry (a $\pi/3$ rotation), we see that $\mathcal{P}_2(q,t) = \mathcal{P}_1(q,t)$.

Let us now consider the class P_3 of r^2-symmetric convex polyominoes with $h_1 = h_2 = h$. In this case, the added decorations on the super-hexagon can only occupy one of the sectors A, B, C or D shown in Figure 14, with the exception of the sectors $A \cap B$ and $C \cap D$ which can be simultaneously occupied.

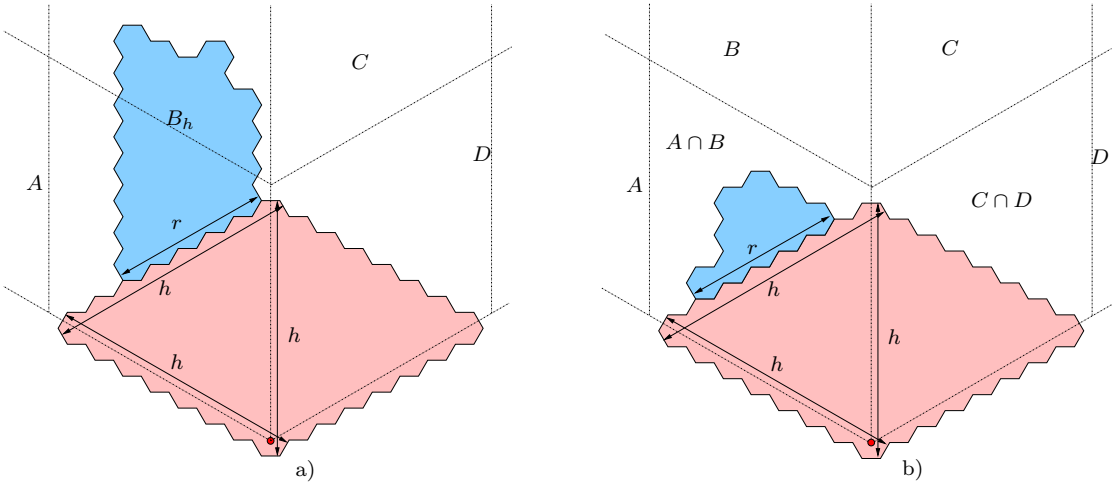

Figure 14: Fundamental regions of r^2-symmetric convex polyominoes in $\mathcal{P}_3$

Denote by B_h the class of admissible decorations in the sector B over an hexagon of *side* h, and by $B_h(q,t)$ its generating series, where the variables q and t mark the added area and half perimeter, respectively. We have

$$B_h(q,t) = \sum_{r=1}^{h-1} \left((h-r)\left(q^r t + \mathcal{D}_{1,r,1}(q,t)\right) + \mathcal{D}_{2,r,1}(q,t) + \sum_{j\geq 2} t^{j-1}\mathcal{D}_{r,j}(q,t) \right) \quad (47)$$

The generating series will be the same for the decorations located in the sectors A, C or D, for symmetry reasons. However, in the term $4B_h(q,t)$, the decorations which, like the one shown in Figure 14b, are located in the intersection sectors $A \cap B$ or $C \cap D$, are counted twice. Observe that these decorations are in fact stack polyominoes of the class T0 with generating series $\mathrm{T0}_{h-1}(t,q)-1$, whence the correcting term $-2(\mathrm{T0}_{h-1}(t,q)-1)$. Lastly, the term $(\mathrm{T0}_{h-1}(t,q)-1)^2$ counts the simultaneous decorations in the sectors $A \cap B$ and $C \cap D$ and the term 1 is added for the empty decoration. Globally, we obtain

$$\mathcal{P}_3(q,t) = \sum_{h\geq 1} t^{3(2h-1)} q^{3h(h-1)+1} \left(4B_h(q^3,t^3) - 4TO_{h-1}(t^3,q^3) + TO^2_{h-1}(t^3,q^3) + 4\right) \qquad (48)$$

5.2.2 The rotation center is on a vertex

The class of r^2-symmetric convex polyominoes whose rotation center is on a vertex is denoted by $\mathcal{Q}$. There are three cases: $h_1 > h_2$, $h_2 > h_1$ and $h_1 = h_2$ to which correspond three series $\mathcal{Q}_1(q,t)$, $\mathcal{Q}_2(q,t)$ and $\mathcal{Q}_3(q,t)$ and two types of central vertices as in Figure 15. The computations

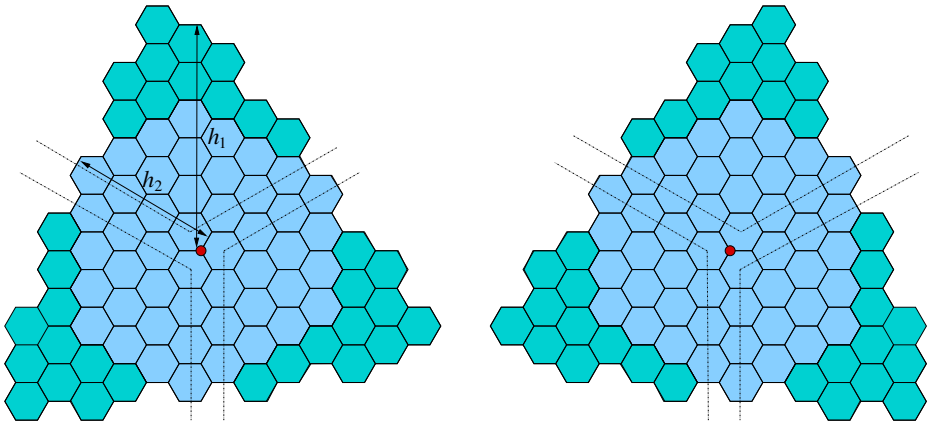

Figure 15: r^2-symmetric convex polyominoes in $\mathcal{Q}_1$

are similar to the preceding case. The decorations are placed over a *pseudo-hexagon* and we find

$$\begin{aligned}\mathcal{Q}_1(q,t) &= 2\sum_{h\geq 1} t^{6h} q^{3h^2} \sum_{l\geq 1}\sum_{r=1}^{h+1}\sum_{s=1}^{h} \frac{1}{q^{3l}} (\mathcal{D}_{0,r,l}(q^3,t^3)\mathcal{D}_{0,s,l}(q^3,t^3) + \mathcal{D}_{0,r,l}(q^3,t^3)\mathcal{D}_{1,s,l}(q^3,t^3) + \\ &\qquad \mathcal{D}_{0,r,l}(q^3,t^3)\mathcal{D}_{2,s,l}(q^3,t^3) + \mathcal{D}_{1,r,l}(q^3,t^3)\mathcal{D}_{1,s,l}(q^3,t^3) + \\ &\qquad \mathcal{D}_{1,r,l}(q^3,t^3)\mathcal{D}_{0,s,l}(q^3,t^3) + \mathcal{D}_{2,r,l}(q^3,t^3)\mathcal{D}_{0,s,l}(q^3,t^3)) \qquad (49) \\ &= \mathcal{Q}_2(q,t)\end{aligned}$$

and

$$\begin{aligned}\mathcal{Q}_3(q,t) &= 2\sum_{h\geq 1} t^{6h} q^{3h^2} \left(4 + 2B_h(q^3,t^3) + 2B_{h+1}(q^3,t^3) - 2TO_{h-1}(t^3,q^3)\right. \\ &\qquad \left. -2TO_h(t^3,q^3) + TO_{h-1}(t^3,q^3)TO_h(t^3,q^3)\right). \qquad (50)\end{aligned}$$

5.2.3 Global result

Finally,

$$|\mathrm{Fix}(\mathrm{r}^2)|_{q,t} = 2\mathcal{P}_1(q,t) + \mathcal{P}_3(q,t) + 2\mathcal{Q}_1(q,t) + \mathcal{Q}_3(q,t). \tag{51}$$

5.3 Symmetry with respect to the π radian rotation r^3

Here, the rotation center can be in the middle of an edge or of an hexagon. See Figure 16. If the

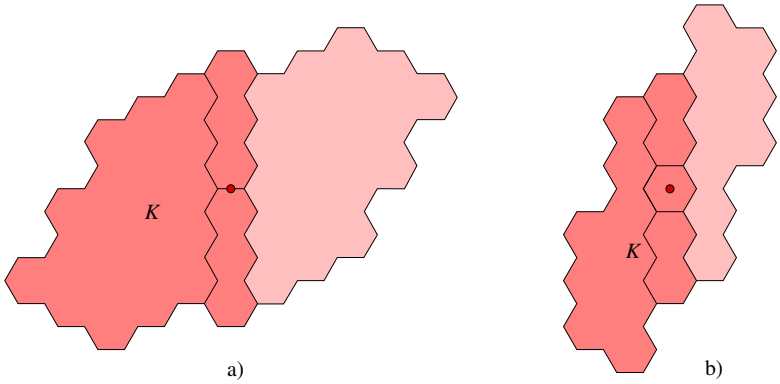

Figure 16: r^3-symmetric convex polyominos

rotation center is in the middle of an edge, there are three similar cases corresponding to the three types of edges. Consider the case of the horizontal edge and denote by $\mathcal{A}$, the corresponding class. Such a polyomino P is shown in Figure 16a. Denote by K the left fundamental region of P, including the central column. Note that this column is of even length.

If the rotation center is the middle of an hexagon, we denote by $\mathcal{H}$ the corresponding class. In this case, the central column is of odd length. See Figure 16b. The polyominoes K which can occur as a fundamental region in one of these two cases are

$$K = C_{00} + C_{01} + C_{10} + C_{11} + C_{02} + C_{20}. \tag{52}$$

Recall that the series $C_{ij,n}(x,q,t)$ is defined by equation (25), with the index n representing the size of the last column. We then have

$$\mathcal{A}(x,q,t) = \sum_{k\geq 1} \frac{1}{xq^{2k}t^{4k+1}}(C_{00,2k} + 2C_{01,2k} + C_{11,2k} + 2C_{02,2k})(x^2,q^2,t^2). \tag{53}$$

and

$$\mathcal{H}(x,q,t) = \sum_{k\geq 0} \frac{1}{xq^{2k+1}t^{4k+3}}(C_{00,2k+1} + 2C_{01,2k+1} + C_{11,2k+1} + 2C_{02,2k+1})(x^2,q^2,t^2). \tag{54}$$

Finally,

$$|\mathrm{Fix}(\mathrm{r}^3)|_{q,t} = 3\mathcal{A}(1,q,t) + \mathcal{H}(1,q,t). \tag{55}$$

6 Two generator symmetry classes

6.1 Symmetry with respect to D_6

Since $D_6 =< \mathrm{r}, \mathrm{ds}_2 >$, convex polyominoes belonging to $\mathrm{Fix}(\mathcal{D}_6)$ consist of super-hexagons with symmetric stack decorations (see the section 5.1). We obtain

$$|\mathrm{Fix}(D_6)|_{q,t} = \sum_{h\geq 1} t^{3(2h-1)} q^{3h(h-1)+1} \mathrm{TS0}_{h-1}(t^6, q^6). \tag{56}$$

6.2 Symmetry with respect to $F_{3,1} =< \mathrm{r}^2, \mathrm{ds}_2 >$

We are guided by the $2\pi/3$ rotation symmetry class studied in section 5.2. The cases $h_1 > h_2$ and $h_2 > h_1$ are impossible because of the ds_2-symmetry. There remains the case $h_1 = h_2 = h$. If the rotation center is in the middle of an hexagon (case $\mathcal{P}_3$), the sides of the superhexagon are decorated by symmetric stacks of type TS0. Moreover the ds_2-symmetry implies that the decorations are in the sectors $A \cap B$ and $C \cap D$. By r^2-symmetry, three of these stacks are identical and the three others also, whence the formula $(TSO_{h-1}(t^3, q^3))^2$. If the rotation center is a vertex (case $\mathcal{Q}_3$), we rather find $TSO_{h-1}(t^3, q^3)TSO_h(t^3, q^3)$. Consequently,

$$\begin{aligned} |\mathrm{Fix}(F_{3,1})|_{q,t} &= \sum_{h\geq 1} t^{3(2h-1)} q^{3h(h-1)+1} (TSO_{h-1}(t^3, q^3))^2 + \\ &\qquad 2\sum_{h\geq 1} t^{6h} q^{3h^2} TSO_{h-1}(t^3, q^3) TSO_h(t^3, q^3). \end{aligned} \tag{57}$$

6.3 Symmetry with respect to $H_{3,1} =< \mathrm{r}^2, \mathrm{v} >$

We refer again to section 5.2. The case where the center is a vertex is impossible because of the vertical symmetry. There remains the case where the center is an hexagon and the three subcases $h_1 > h_2$, $h_2 > h_1$ and $h_1 = h_2$ define three subclasses $\mathcal{R}_1$, $\mathcal{R}_2$ and $\mathcal{R}_3$, respectively. For the case where $h_1 > h_2$, the part D^* of the decoration (see Figure 13) is in fact the mirror image $\mathrm{v} \cdot D$ of D. Hence we obtain

$$\begin{aligned} \mathcal{R}_1(q,t) &= \sum_{h\geq 1} t^{3(2h-1)} q^{3h(h-1)+1} \sum_{l\geq 1} \sum_{r=1}^{h} \frac{1}{q^{3l}} \left(C_{0,r,l}(q^6, t^6) + C_{1,r,l}(q^6, t^6) \right) \\ &= \mathcal{R}_2(q,t). \end{aligned} \tag{58}$$

If $h_1 = h_2 = h$, the decorations in the sectors $A \cap B$ and $C \cap D$ are mirror images of each other and we find

$$\mathcal{R}_3(q,t) = \sum_{h\geq 1} t^{3(2h-1)} q^{3h(h-1)+1} \mathrm{T0}_{h-1}(t^6, q^6). \tag{59}$$

Finally,

$$|\mathrm{Fix}(H_{3,1})|_{q,t} = 2\mathcal{R}_1(q,t) + \mathcal{R}_3(q,t). \tag{60}$$

6.4 Symmetry with respect to $D_{2,3} =< \mathrm{r}^3, \mathrm{h} >$

Observe that $D_{2,3} =< \mathrm{h}, \mathrm{v} >$. We thus refer to sections 4.1 and 4.2 on v- and h-symmetric polyominoes, respectively. In order to obtain a $D_{2,3}$-symmetric convex polyomino, it suffices to take a v-symmetric polyomino whose fundamental region K (see the figure 11) is itself h-symmetric.

The series $\mathrm{CS}_{00}(x,q,v,t)$, $\mathrm{HS}_{11}(x,q,u,v,t)$ and $\mathrm{CS}_{11}(x,q,v,t)$ are the h-symmetric analogues of the series $C_{00}(x,q,v,t)$, $H_{11}(x,q,u,v,t)$ and $C_{11}(x,q,v,t)$ of sections 2.3.4 and 3.1. We have

$$\mathrm{CS}_{00,k}(x,q,t) = [v^k]\mathrm{CS}_{00}(x,q,v,t) = t^{2k}\mathrm{TS}_k(xt,q), \tag{61}$$

$$\begin{aligned}\mathrm{HS}_{11}(x,q,u,v,t) &= \frac{xquvt^3}{1-quvt^2} + xqvt^3\ \mathrm{HS}_{11}(x,q,u,vq,t) + \\ &\qquad \frac{xt}{qv}\left(\mathrm{HS}_{11}(x,q,u,vq,t) - v(\frac{\mathrm{HS}_{11}(x,q,u,v,t)}{v})_{v=0}\right) \\ &= \sum_{k\geq 1}\mathrm{HS}_{11,k}(x,q,v,t)u^k,\end{aligned} \tag{62}$$

$$\begin{aligned}\mathrm{CS}_{11}(x,q,v,t) &= \sum_{i\geq 2}\frac{1}{t^{2i-2}}\mathrm{CS}_{00,i}(x,q,t)\mathrm{HS}_{11,i-1}(x,q,v,t) \\ &= \sum_{k\geq 1}\mathrm{CS}_{11,k}(x,q,t)v^k,\end{aligned} \tag{63}$$

and finally

$$|\mathrm{Fix}(D_{2,3})|_{q,t} = \sum_{i\geq 1}\frac{1}{q^i t^{2i+1}}\left(\mathrm{CS}_{00,i}(1,q^2,t^2) + \mathrm{CS}_{11,i}(1,q^2,t^2)\right). \tag{64}$$

7 Conclusion

It is now possible to use Burnside's formula (12), with $\mathcal{F} = C$, to enumerate the free convex polyominoes, according to area and half perimeter. Some numerical results are given in tables 1 and 2, according to area only (up to area 20) or to half perimeter only (up to half perimeter 16). See under the column "Orbits".

It is also possible to enumerate asymmetric convex polyominoes with the help of formula (16), with $\mathcal{F} = C$. Some results are found in the tables 1 and 2. It is clear on these tables that almost all convex polyominoes are asymmetric.

All these numerical results were verified experimentally by an exhaustive computerized enumeration.

References

[1] Mireille Bousquet-Mélou. A method for the enumeration of various classes of column-convex polygons. *Discrete Mathematics*, 154:1–25, 1996.

Table 1: Symmetry classes of convex (hexagonal) polyominoes according to area

Area	id	h	v	r	r^2	r^3	Orbits	$\mathcal{D}_6$	F_{31}	H_{31}	D_{21}	Asym
1	1	1	1	1	1	1	1	1	1	1	1	0
2	3	1	1	0	0	3	1	0	0	0	1	0
3	11	3	3	0	2	3	3	0	2	0	1	0
4	38	2	4	0	2	12	6	0	0	2	2	24
5	120	6	10	0	0	12	15	0	0	0	2	72
6	348	6	12	0	6	42	38	0	2	0	2	264
7	939	9	27	1	3	37	91	1	1	3	3	816
8	2412	12	30	0	0	126	222	0	0	0	4	2184
9	5973	17	63	0	12	99	528	0	0	0	3	5640
10	14394	20	66	0	6	336	1250	0	2	4	4	13836
11	34056	30	142	0	0	252	2902	0	0	0	6	33324
12	79602	38	140	0	18	840	6751	0	2	0	4	78240
13	184588	46	310	1	13	616	15525	1	1	5	8	182952
14	426036	62	286	0	0	2028	35759	0	0	0	8	423012
15	980961	69	665	0	30	1461	82057	0	2	0	7	977316
16	2256420	100	580	0	18	4788	188607	0	0	6	8	2249640
17	5189577	115	1441	0	0	3435	433140	0	0	0	11	5181540
18	11939804	154	1184	0	50	11142	996255	0	2	0	12	11924676
19	27485271	175	3145	1	27	8005	2291941	1	1	7	13	27467376
20	63308532	238	2458	0	0	25800	5278535	0	0	0	16	63274740

[2] A. Denise, C. Dürr, and F. Ibn-Majdoub-Hassani. Enumération et génération aléatoire de polyominos convexes en réseau hexagonal. In *Proceedings of the 9th Conference on Formal Power Series and Algebraic Combinatorics (FPSAC'97)*, pages 222–234, Universität Wien, 1997.

[3] Dominique Gouyou-Beauchamps et Pierre Leroux. Dénombrement des classes de symétries des polyominos hexagonaux convexes. In *Proceedings of the 16th Conference on Formal Power Series and Algebraic Combinatorics (FPSAC'04)*, University of British Columbia, Canada, 2004.

[4] S. Feretić and D. Svrtan. On the number of column-convex polyominoes with given perimeter and number of columns. In *Proceedings of the 5th Conference on Formal Power Series and Algebraic Combinatorics (FPSAC'93)*, pages 201–214, University of Florence, 1993.

[5] A. J. Guttmann and I. G. Enting. The number of convex polygons on the square and honeycomb lattices. *J. Phys. A: Math. Gen.*, 21:L467–L474, 1988.

[6] F. Ibn-Majdoub-Hassani. Combinatoire des polyominos et des tableaux décalés oscillants. PhD Thesis, Université de Paris Sud, Orsay, November 1996.

[7] P. Leroux and É. Rassart. Enumeration of symmetry classes of parallelogram polyominoes. *Ann. Sci. Math. Québec*, 25(1):71–90, 2001.

[8] P. Leroux, É. Rassart, and A. Robitaille. Enumeration of symmetry classes of convex polyominoes in the square lattice. *Advances in Applied Mathematics*, 21:343–380, 1998.

[9] K. Y. Lin and S. J. Chang. Rigorous results for the number of convex polygons on the square and honeycomb lattices. *J. Phys. A: Math. Gen.*, 21:2635–2642, 1988.

Table 2: Symmetry classes of convex (hexagonal) polyominoes according to half perimeter

$\frac{1}{2}$per.	id	h	v	r	r^2	r^3	Orbits	$\mathcal{D}_6$	F_{31}	H_{31}	D_{21}	Asym
3	1	1	1	1	1	1	1	1	1	1	1	0
4	0	0	0	0	0	0	0	0	0	0	0	0
5	3	1	1	0	0	3	1	0	0	0	1	0
6	2	2	0	0	2	0	1	0	2	0	0	0
7	12	2	4	0	0	6	3	0	0	0	2	0
8	18	2	0	0	0	0	2	0	0	0	0	12
9	59	5	9	1	5	19	11	1	3	3	3	24
10	120	8	0	0	0	0	12	0	0	0	0	96
11	318	10	24	0	0	48	39	0	0	0	6	204
12	714	14	0	0	12	0	65	0	4	0	0	672
13	1743	25	59	0	0	129	177	0	0	0	7	1368
14	4008	36	0	0	0	0	343	0	0	0	0	3900
15	9433	53	143	2	28	323	867	2	6	8	15	8616
16	21672	76	0	0	0	0	1825	0	0	0	0	21444

[10] K. Y. Lin and F. Y. Wu. Unidirectional convex polygons on the honeycomb lattice. *J. Phys. A: Math. Gen.*, 23:5003–5010, 1990.

[11] A. J. Guttmann M. Vöge and I. Jensen. On the number of benzenoid hydrocarbons. *J. Chem. Inf. Comput. Sci.*, 42:456–466, 2002.

[12] V. Privman and N. M. Švrakić. *Directed Models of Polymers, Interfaces, and Clusters: Scaling and Finite-Size Properties*. Lecture Notes in Physics, Springer-Verlag, Volume 338, 1989.

[13] N. J. A. Sloane. *The On-Line Encyclopedia of Integer Sequences*. Published electronically at `http://www.research.att.com/~njas/sequences/`, 2003.

[14] N. J. A. Sloane and S. Plouffe. *The Encyclopedia of Integer Sequences*. Academic Press, Inc., 1995.

[15] P. K. Stockmeyer. Enumeration of graphs with prescribed automorphism group. Ph.D. Thesis, University of Michigan, Ann Arbor, 1971.